

Fusion of LIDAR Data and Large-scale Vector Maps for Building Reconstruction

Liang-Chien Chen¹, Chih-Yi Kuo², Jiann-Yeou Rau³, Chi-Heng Hsieh⁴
Professor¹, Student², Specialist³, Student⁴

Center for Space and Remote Sensing Research
National Central University, Chung-Li, TAIWAN

lcchen@csrnr.ncu.edu.tw; 92322096@cc.ncu.edu.tw; jyrau@csrnr.ncu.edu.tw; 93322082@cc.ncu.edu.tw

Abstract: LIDAR data contains plenty of height information, while vector maps preserve accurate building boundaries. From the viewpoint of data fusion, we integrate LIDAR data and large-scale vector maps to perform building modeling. The proposed scheme comprises six major steps: (1) preprocessing of LIDAR data and vector maps, (2) extraction of point clouds that belong to a building, (3) construction of the facets from the point clouds, (4) detection of planar faces, (5) determination of 3-D edges of buildings, and (6) regularization of 3-D edges and building reconstruction. In the preprocessing stage, the height variation of the aboveground objects is extracted by subtracting the surface elevation from the terrain. The polygons for buildings are also obtained from the polylines using the SMS method. Using the vertex locations and rough heights of stories, the point clouds that belong to a building can be selected. Then a triangulated irregular network is built for representing the facets of the point clouds. Segmentation of planar faces is implemented by examining the size and the angles among surface normal vectors. After detection for planar roof faces, 3-D roof edges are determined by intersecting roof planes. Finally, building models are reconstructed after regularization.

Keywords: LIDAR, Vector Maps, Building Reconstruction, Triangulated Irregular Network.

1. Introduction

In response to the development of 3D spatial information for urban planning and management, cyber city modeling is getting important. In the cyber space, the information of the real world is stored and reconstructed in the computer system. The applications of the cyber city are essential, such as in the map revision, change detection, transportation, urban planning, environmental planning [1], flight simulations [2], etc. Because the cyber city is a replica of the real world, the information provides valuable decision support to city managers.

Building models, among others, could be the most important elements in a cyber city. Thus, building modeling becomes an important task in photogrammetry and GIS areas. Building reconstruction may be accomplished by two strategies, i.e., fully automatic approach and semi-automatic approach. Fully automation is always an ultimate goal. However, it is difficult to achieve automatic interpretation, many researches aim at semi-automatic method in the model production [3][4].

Building models may be reconstructed by using aerial photography [5] such as using CSG model-image fitting [6]. Some investigations integrate aerial photos and LIDAR data to reconstruct building models [7]. Due to its maturity, LIDAR (light detecting and ranging) has demonstrated profound potentials in automatic building reconstruction. Many researches reported the results of using LIDAR point clouds to reconstruct buildings [8][9][10][11]. Although the results are encouraging, the applicability of those methods is limited to simple buildings. LIDAR data contains plenty of height information, while vector maps preserve accurate building boundaries. From the viewpoint of data fusion, we integrate LIDAR data and large-scale vector maps to perform modeling for complex buildings. The workflow of investigation is shown in Fig. 1.

2. Data Preprocessing

The procedure starts from the resampling the LIDAR point clouds into grid form. Then the height variations of the above ground objects are extracted by subtracting the ground elevation from the surface points.

In the part of vector maps, because there is no topology among building boundaries in the line maps, closed polygons are built from polylines by using the SMS method [12]. The rough heights of stories are also obtained and associated with building polygons.

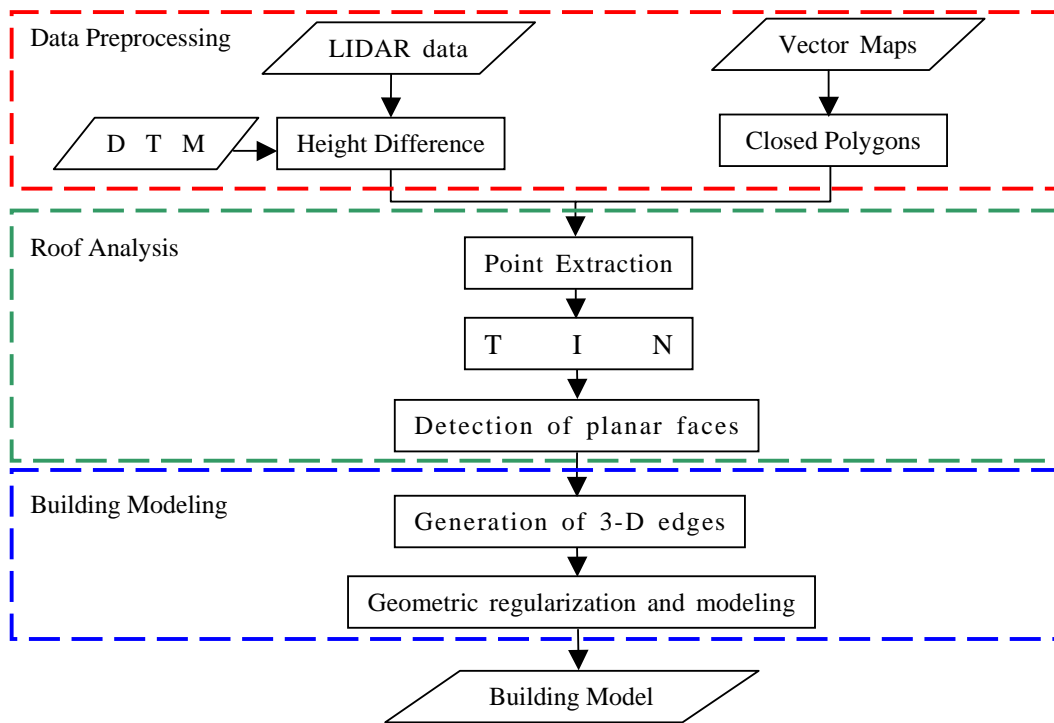


Figure 1. Workflow of the proposed scheme

3. Roof Analysis

In this stage, point clouds inside the building boundaries are selected first. Then the point clouds are organized with a TIN (Triangular Irregular Network) structure. Finally, the detection of planar faces is taken using region growing approach.

1) Point Extraction

In order to avoid selecting the erroneous points, point clouds have to be located inside the polygon and having the height closed to the one indicated in the vector maps with the number of stories. The point-in-polygon technique [14] is taken to select points inside the polygon. Using the vertex locations and rough heights of stories, the point clouds that belong to a building can be extracted.

2) Construction of Triangular Irregular Network (TIN)

A triangulated irregular network is built for representing the facets of the point clouds by using Delaunay triangulation [13]. It is done in such a way that the successive processes could remain high fidelity.

3) Detection of planar faces

In this step, we implement the planar analysis for the roofs and the walls. It is an important step to determine the roof surfaces. Considering the buildings with step edges, the detection of wall faces is also included in this step. The region growing and direct segmentation are two commonly used methods in planar analysis. The first method starts from a seed element then searches adjacent elements to determine if the characteristics are similar to the seed. The seed region grows as long as the adjacent elements behave similarly. When a region stops growing, a new seed element will be chosen. The region growing stops when all elements are assigned. The second method computes geometric parameters of all elements followed by the detection of planar faces using clustering technique [15].

In this investigation, we select the region growing approach. Angles among surface normal vectors and the minimum area are chosen as the geometric parameters for roof surfaces. The height differences, in addition to the two previous parameters, are also analyzed in the wall face determination.

Once the point clouds that belong to a building are selected, a triangulated irregular network is built. The surface normal vector of each triangle is determined first. Starting from a seed triangle, if the normal vectors of the seed and its neighboring triangle have similar orientation, those two triangles are combined. The seed region grows as long as the angle difference between two adjacent triangles is under a threshold. The reference surface normal vector is recalculated using the normal vectors of all triangles that belong to the region. A new seed triangle is chosen when the region stops growing. The region-growing step stops when all triangles have been assigned as roofs or walls. Due to the errors of the LIDAR data, those detected regions may consist fragmental triangles. Thus, small regions will be merged with its neighborhood that has the closest normal vector.

4. Building Modeling

1) Determination of 3-D Edges

After detecting roof surfaces and wall faces, three kinds of 3-D edges are generated. The first kind is computed by the intersection of two adjacent planar faces. The second one, called the step edge, is determined by examining the orthogonal vector of a wall region. The third kind of edges is computed from the intersection of the building boundary and the detected edges.

2) 3-D Edges Regularization and Building Reconstruction

In this investigation, 3-D edges are regularized employing geometric constraints. In which the end points of edges are adjusted to the most probable locations by least squares adjustment. There are three steps: (1) selection of suitable geometric condition, (2) forming the observation equations, and (3) determination of unknown parameters by least squares adjustment.

Four geometric constraints are considered according to the characteristic of general buildings: (i) 3-D edges are either parallel or orthogonal to the principal axis of a building, (ii) a roof edge is horizontal if the end points have similar elevations, (iii) a middle point is selected if an intersection point is close to the middle of an edge, (iv) end points of 3-D edges which form a roof surface are coplanar. The four geometric constraints are then used in the least squares solution to adjust end points of 3-D edges. Fig. 2(a), 2(b), 2(c), and 2(d) represent the four constraints, respectively.

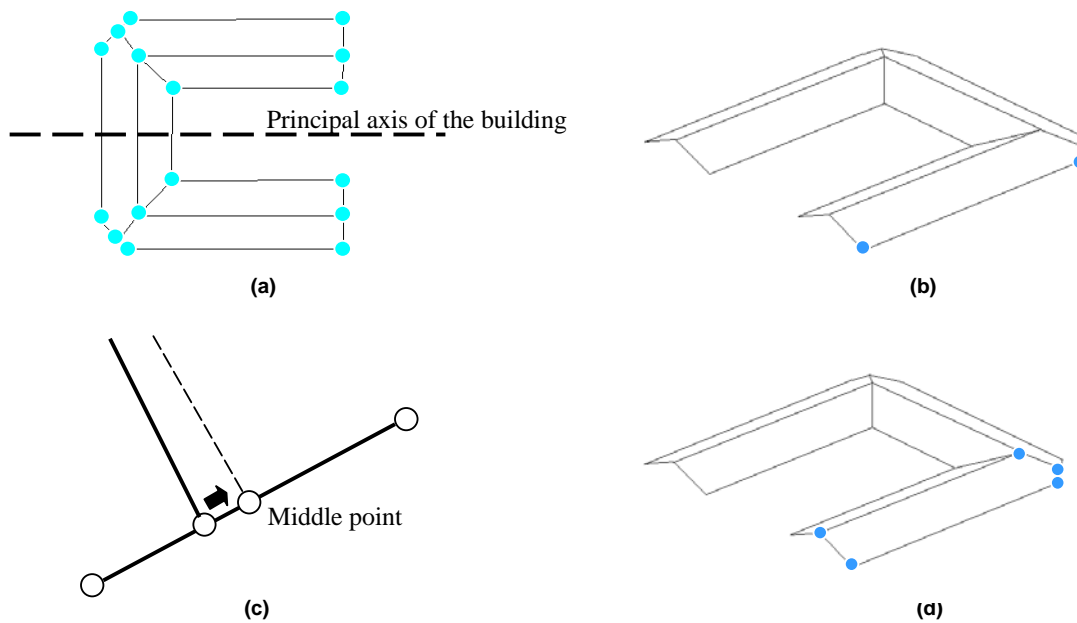


Figure 2. Geometric constraints for building regularization
 (a) Principal axis constraint, (b) Horizontal constraint, (c) Symmetric constraint, (d) Coplanar constraint

Polyhedral models are considered in this investigation. In this manner, planar faces are appropriate to describe the surface of a house roof. After regularizing the 3-D edges, building models are reconstructed by using SMS method [7].

5. Experiment and Results

Acquired by an Optech ALTM, the LIDAR data used in this research is located in Tai-Chung city of central Taiwan. The test area contains 115 buildings. The discrete LIDAR points were classified into vegetation points and ground points. The average density of LIDAR data is about 1.71 points per square meter. The vertical accuracy of the point clouds is about 0.15m. The used vector maps are with a scale of 1:1,000.

In the first step, the ground points from LIDAR data are resampled into a grid DEM with a pixel size of 1m. Fig.3 shows the results of the height variation of the aboveground objects, called nDSM(normalized DSM), which is determined by subtracting the surface elevation from the DEM.

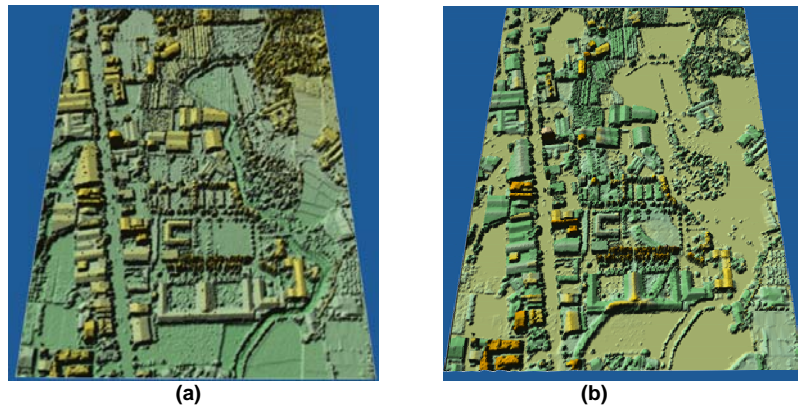


Figure 3. Steps of preprocessing of LIDAR data, (a) DSM, (b) nDSM

According to the shape complexity, we categorize the buildings into four types: (1) buildings with horizontal roofs, (2) buildings with ridged lines in the single direction, (3) buildings with ridged lines in different directions, and (4) buildings with camber roofs. Fig. 4 shows the examples of the four kinds of buildings. The numbers of each type of buildings are also indicated.





Horizontal roof buildings : 36		Simple gable roof buildings : 53	
			
Complex gable roof buildings : 19		Camber roof buildings : 6	
			

Figure 4. Four types of test buildings

Some selected examples with different building complexities are given in the following. Fig. 5 illustrates a group of simple buildings that are the ones with horizontal roofs and simple gable roofs. The reconstruction procedure for a

complex building with multiple gable roofs is gives in Fig. 6. Fig. 6(a) is the results of the detection for planar faces. Three-dimensional edges before and after the regularization are shown in Fig. 6(b) and 6(c), respectively. Fig. 6(d) illustrates the reconstructed building. Fig. 7 demonstrates a building with multiple gable roofs and step edges. The results of the detection for planar faces are shown in Fig. 7(a). Fig. 7(b) illustrates the successfully reconstructed building. Fig. 8(a) is for the demonstration for the buildings with camber roofs. It is observed that the camber roofs, as shown in Fig. 8(b), are resulted in a group of gable buildings. The phenomenon is due to the limitation of the polyhedral model that we select in the investigation. The improvements of the proposed scheme are thus needed for this kind of building.

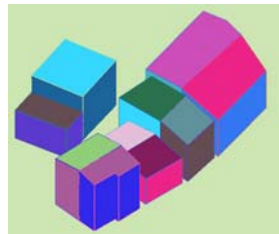


Figure 5. Examples of reconstructed simple buildings

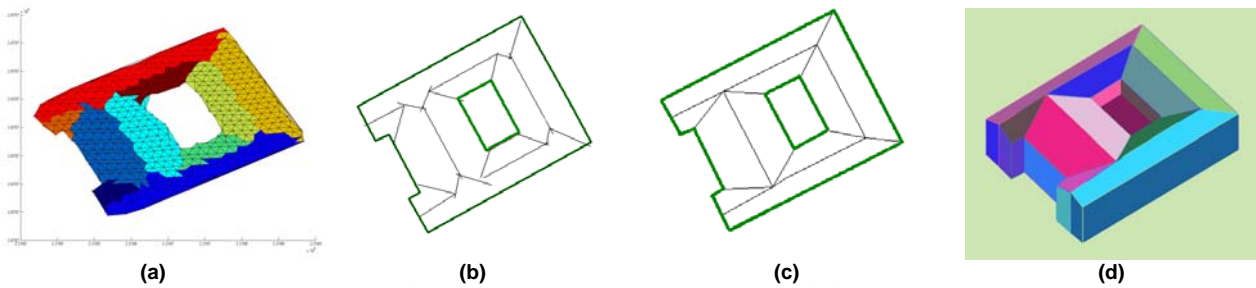


Figure 6. Results of complex gable roof building.

(a) Results of detection for planar faces, (b) Computed 3-D edges, (c) 3-D edges after regularization, (d) Reconstructed 3-D building model

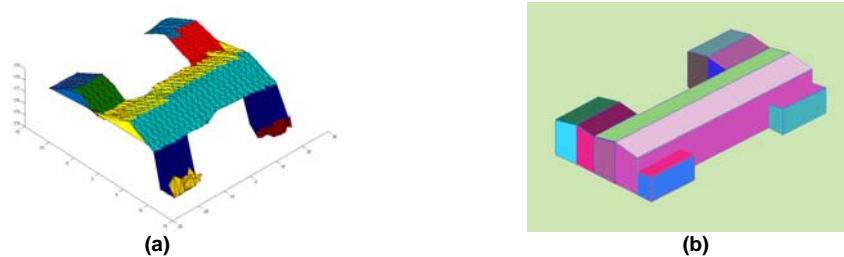


Figure 7. Results of a complex building with multiple gable roofs and step edges,
(a) Results of detection for planar faces, (b) Reconstructed 3-D building model

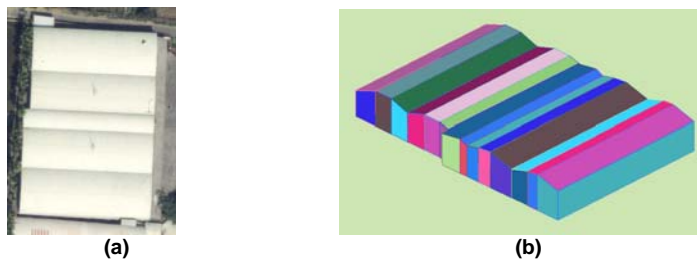


Figure 8. Result of camber roof building, (a) Aerial image, (b) Reconstructed 3-D building model

The fidelity of the building reconstruction is validated in terms of the successful rate. The successful rate of the reconstruction is divided into three categories, namely, correct, partially correct and erroneous. Those reconstructed buildings that have the same shape with the real ones are called correct. The category of the partially correct is for a

group of connected buildings when a part is successfully reconstructed. The reconstruction is erroneous when the building model is different, in shape, with the real one. Table 1 shows the successful rate for the four kinds of buildings. Building models in the entire test area are shown in Fig. 9. One hundred and three out of one hundred and fourteen buildings have been correctly reconstructed. The buildings that failed in the reconstruction, i.e., the erroneous category, are the ones that do not have sufficient point clouds on the roof. The mean value of height differences between LIDAR points and roof surface, called shaping error, is 0.171 m. The discrepancies range from 0.004 m to 0.341 m.

Table 1. Successful rate of building reconstruction

Reconstruction results	Horizontal roof	Simple gable roof	Complex gable roof	Camber roof	Successful rate
Correct	36	53	8	6	90%
Partially correct	0	0	9	0	8%
Erroneous	0	0	2	0	2%

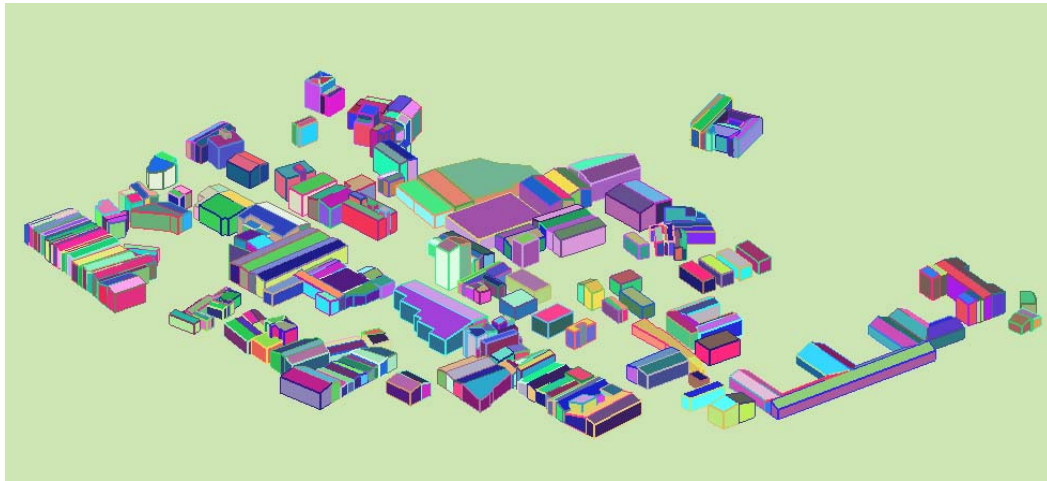


Figure 9. Results of building models in the test area

6. Conclusions

We have presented a scheme for the detection of planar faces and building modeling by the fusion of LIDAR data and large-scale vector maps. The results from the experiment show the potential of the proposed method. Ninety percent of complex buildings are reconstructed successfully by the proposed approach. The proposed method takes the advantage of high horizontal accuracy from vector maps and high vertical accuracy from LIDAR data. The shaping error is 0.171 m, which corresponds to the vertical accuracy of LIDAR data.

Acknowledgement

This investigation was partially supported by the National Science Council of Taiwan under Project No. NSC93-2211-E-008-027. Thanks also go to the Council of Agriculture for providing the test data sets.

References

- [1] Danahy, J., 1999. Visualization data needs in urban environmental planning and design, *Proceedings of the Photogrammetric Week*, Karlsruhe, pp. 351-365.
- [2] VolZ, S. and D. Klinec, 1999. Nexus: the development of a platform for location aware application, *Proceedings of the third Turkish-German Joint Geodetic Days*, Vol. 2, Istanbul, pp. 599-608.

- [3] Lang, F., T. Leoecherbach, W. Schickler, 1995. A one-eye stereo system for semi-automatic 3D-building extraction, *Geomatics Info Magazine*, pp. 1-4.
- [4] Chio, S. H., S. C. Wang, 1999. Semi-automatic system for roof reconstruction based on 3-D linear segments, *Proceedings of the 20th Asian Conference on Remote Sensing*, pp. 165-170.
- [5] Taillendier, F., & R. Deriche, 2004. Automatic building reconstruction from aerial images: a generic Bayesian framework, *IAPRS International Archives of Photogrammetry and Remote Sensing*, Vol. XXXV, part B3, pp. 343-348.
- [6] Tseng, Y. H. and S. Wang, 2003. Semiautomated building extraction based on CSG model-image fitting, *Photogrammetric Engineering & Remote Sensing*, Vol. 69, No. 2, pp. 171-180.
- [7] Rottensteiner, F., 2003. Automatic generation of high-quality building models from LIDAR data, *IEEE Computer Graphics and Applications*, Vol. 23, Issue: 6, pp.42-50.
- [8] Halla, N. and Brenner, C., 1998. Interpretation of urban surface models using 2D building information, *Computer Vision and Image Understanding*, Vol. 72, No. 2, pp. 204-214.
- [9] Vögtle, T. and E. Steinle, 2000. 3D modeling of building using laser scanner and spectral information, *IAPRS International Archives of Photogrammetry and Remote Sensing*, Vol.33, Part B3, pp. 927-934.
- [10] Chen, L. C., Y. C. Lai and J. Y. Rau, 2003. Fusion of LIDAR data and aerial images for building reconstruction, *Proceedings of 24th Asia's Conference on Remote Sensing*, pp. 654-656.
- [11] Hofmann, A. D., 2004. Analysis of TIN-structure parameter spaces in airborne laser scanner data for 3-D building model generation, *IAPRS International Archives of Photogrammetry and Remote Sensing*, Vol. 35, Part B3, pp. 302-307.
- [12] Chen, L. C., and Rau, J. Y., 2003. Robust reconstruction of building models from three-dimensional line segments, *Photogrammetric Engineering & Remote Sensing*, Vol. 69, No. 2, pp. 181-188.
- [13] Golias, N. A. and Dutton, R. W., 1997. Delaunay triangulation and 3D adaptive mesh generation, *Finite Element in Analysis and Design*, Vol. 25, pp. 331-341.
- [14] Mortenson, M. E., 1999. Mathematics for computer graphics application, *Industrial Press*, New York, 2nd edition, pp. 202-204.
- [15] Vosselman, G. and Maas, H. G., 1999. Two algorithms for extracting building model from raw laser altimetry data, *ISPRS journal of Photogrammetry & Remote Sensing*, Vol.54, pp.153-163.